Purinergic Signalling (2022) 18:481–494
https://doi.org/10.1007/s11302-022-09888-w

ORIGINAL ARTICLE

$P2Y_{12}$ receptor antagonism inhibits proliferation, migration and leads to autophagy of glioblastoma cells

Pedro Vargas[1,2] · Thamiris Becker Scheffel[1] · Fernando Mendonça Diz[1] · Liliana Rockenbach[1,2] · Nathália Grave[1,2] · Angélica Regina Cappellari[1] · Luiza Wilges Kist[3,4] · Maurício Reis Bogo[2,3,4] · Marcos Paulo Thomé[5] · Gabriel Fernandes Leal[6] · Amanda de Fraga Dias[7] · Fabrício Figueiró[7] · Eduardo Cremonese Filippi-Chiela[8] · Guido Lenz[5] · Fernanda Bueno Morrone[1,2,3]

Received: 13 April 2022 / Accepted: 21 July 2022 / Published online: 8 August 2022

Abstract

Glioblastoma (GBM) is the most aggressive and lethal among the primary brain tumors, with a low survival rate and resistance to radio and chemotherapy. The $P2Y_{12}$ is an adenosine diphosphate (ADP) purinergic chemoreceptor, found mainly in platelets. In cancer cells, its activation has been described to induce proliferation and metastasis. Bearing in mind the need to find new treatments for GBM, this study aimed to investigate the role of the $P2Y_{12}R$ in the proliferation and migration of GBM cells, as well as to evaluate the expression of this receptor in patients' data obtained from the TCGA data bank. Here, we used the $P2Y_{12}R$ antagonist, ticagrelor, which belongs to the antiplatelet agent's class. The different GBM cells (cell line and patient-derived cells) were treated with ticagrelor, with the agonist, ADP, or both, and the effects on cell proliferation, colony formation, ADP hydrolysis, cell cycle and death, migration, and cell adhesion were analyzed. The results showed that ticagrelor decreased the viability and the proliferation of GBM cells. $P2Y_{12}R$ antagonism also reduced colony formation and migration potentials, with alterations on the expression of metalloproteinases, and induced autophagy in GBM cells. Changes were observed at the cell cycle level, and only the U251 cell line showed a significant reduction in the ADP hydrolysis profile. TCGA data analysis showed a higher expression of $P2Y_{12}R$ in gliomas samples when compared to the other tumors. These data demonstrate the importance of the $P2Y_{12}$ receptor in gliomas development and reinforce its potential as a pharmacological target for glioma treatment.

Keywords Glioblastoma · Purinergic system · $P2Y_{12}$ receptor · ADP · Ticagrelor

✉ Fernanda Bueno Morrone
fernanda.morrone@pucrs.br; fbmorrone@gmail.com

[1] Laboratório de Farmacologia Aplicada, Escola de Ciências da Saúde e da Vida, Pontifícia Universidade Católica do Rio Grande do Sul, Porto Alegre, RS, Brazil

[2] Programa de Pós-Graduação em Medicina e Ciências da Saúde, Pontifícia Universidade Católica do Rio Grande do Sul, Porto Alegre, RS, Brazil

[3] Programa de Pós-Graduação em Biologia Celular e Molecular, Pontifícia Universidade Católica do Rio Grande do Sul, Porto Alegre, RS, Brazil

[4] Laboratório de Biologia Genômica e Molecular, Escola de Ciências da Saúde e da Vida, Pontifícia Universidade Católica do Rio Grande do Sul, Porto Alegre, RS, Brazil

[5] Departamento de Biofísica, Instituto de Biociências, Universidade Federal do Rio Grande do Sul, Porto Alegre, RS, Brazil

[6] Programa de Pós-Graduação em Ciência da Computação, Escola Politécnica, Pontifícia Universidade Católica do Rio Grande do Sul, Porto Alegre, RS, Brazil

[7] Departamento de Bioquímica, Instituto de Ciências Básica da Saúde, Universidade Federal Do Rio Grande Do Sul, Porto Alegre, RS, Brazil

[8] Departmento de Ciências Morfológicas, Instituto de Ciências Básicas da Saúde, Universidade Federal Do Rio Grande Do Sul, Porto Alegre, RS, Brazil

Pedro Vargas graduated in Pharmacy from the Pontifical Catholic University of Rio Grande do Sul. Master in Cellular and Molecular Biology from the Pontifical Catholic University of Rio Grande do Sul and PhD in Medicine and Health Sciences, with emphasis in Pharmacology and Biochemistry from the Pontifical Catholic University of Rio Grande do Sul. He has experience in the areas of cancer, nanotechnology, cosmetology and lipid drug delivery systems.

Introduction

Gliomas are the most common malignant tumors of the central nervous system (CNS) [1, 2] and they have been related to most deaths from primary brain tumors, presenting very limited forms of treatment [3, 4]. The World Health Organization (WHO) classified gliomas into four grades (I–IV) based on their morphology, increased mitotic activity, and histopathological characteristics [5]. Recently, these tumors have been divided into different subclasses according to genetic alterations, and expression profiles mainly of platelet-derived growth factor receptor alfa (PDGFRA), epidermal growth factor receptor (EGFR), neurofibromatosis 1 (NF1), and isocitrate dehydrogenase 1 and 2 (IDH1 and IDH2) [6].

Glioblastoma (GBM) is the most aggressive type of glioma, and the prognosis gets worse as age increases [1, 7]. For more than three decades, postoperative radiotherapy has been the standard treatment for newly diagnosed GBM [8]. Besides, temozolomide (TMZ), an alkylating agent, is widely used in the treatment of GBM, reducing the risk of recurrence and prolonging patients' survival, despite bringing important adverse effects, such as hematological toxicity, thrombocytopenia, and lymphopenia [9].

The development of GBM as well as their invasive behavior is tightly controlled by the local microenvironment. Molecules found in the extracellular milleu, such as adenosine triphosphate (ATP), adenosine diphosphate (ADP), and adenosine, have been described to stimulate GBM invasion changing the local microenvironment to favor tumor progression [10, 11].

The purinergic signaling is based on cellular ATP release, and subsequent binding to purine receptors in the extracellular space, modulating its functions [12]. In the tumor microenvironment, due to inflammation and the presence of hypoxia in solid tumors, both ATP and adenosine may be kept elevated for extended periods of time [13]. It is well established that malignant tumors promote a strong inflammatory response and are characterized by the presence of necrotic areas with ATP release [14].

In this context, ATP and other nucleotides have effects on the tumor cells by stimulation of P2Y purinergic receptors [15]. Among these, the metabotropic $P2Y_{12}$ receptor ($P2Y_{12}R$) recognizes ADP as its ligand. It is coupled to Gi protein and is highly expressed in platelets, presenting an important role in the coagulation process, vascular smooth muscle, and brain [16]. Also, ADP activates the $P2Y_{12}R$ in microglial cells to induce chemotaxis, serving as a "detector" signal, and $P2Y_{12}$ antagonists can be targets for inflammatory and chronic neuropathic pain control [17]. This receptor is overexpressed in C6 glioma cells and is localized also, along with other purinergic receptors such as $P2Y_1$ and $P2Y_2$ [18].

Among the $P2Y_{12}$ antagonists, thienopyridines comprising ticlopidine, clopidogrel, and prasugrel are well-known antithrombotic drugs and irreversibly inhibit $P2Y_{12}$ upon metabolic conversion into active metabolites by the hepatic cytochrome P-450 system [19]. Ticagrelor, on the other hand, does not require biotransformation to become an active drug. Its mechanism of action is based on the binding on an allosteric site of the $PY_{12}R$, therefore, the endogenous agonist ADP can bind to the receptor, but it is not able to perform its biological effects [20].

In view of the expression of the $P2Y_{12}R$ in glioma cells, we evaluated if the antagonism of $P2Y_{12}R$, through the antiplatelet drug ticagrelor, can alter the proliferation and the migratory profile of GBM cells.

Materials and methods

Cell cultures and treatments

The human GBM cell line (U251) is from the ATCC (Rockville, MD, USA) and the patient-derived GBM cells (LS12) were previously obtained as described by Kipper et al. (2018). Briefly, LS12 cells come from a female patient submitted to surgical resection at São Lucas Hospital from PUCRS, with a diagnosis at 44 years, obtaining confirmation of grade IV glioma through histopathological analysis [21].

This study was conducted in accordance with the appropriate guidelines and ethical protocols (Ethical Committee approval protocol at UFRGS: 420.856 and at PUCRS: 429.849) and after obtaining informed consent from the patient. U251 cells were maintained in Dulbecco's modified Eagle medium (DMEM) while LS12 cells were cultivated in DMEM-F12, both supplemented with 10% fetal bovine serum (FBS), under ideal culture conditions and kept in a humidified cell incubator (37 °C, 5% CO_2, 95% humidity). Upon reaching semi-confluence, cells were treated with the $P2Y_{12}$ receptor agonist, ADP (100 µM), with the antagonist, ticagrelor, at different concentrations (5, 10, 20, 50, 100, 200 µM) or $P2Y_1$ antagonist, MRS2179, at different concentrations (5, 10, 20, 50 µM). Treatments were carried out within 24 h for the purpose of performing a time versus response curve with ticagrelor in solution and ADP.

Gene expression

U251 ($n=4$) and LS12 ($n=4$) were seeded in 6-well plates. After 24 h, the total RNA from cells was isolated using Trizol LS reagent (Invitrogen, Carlsbad, CA, USA). The cDNA was synthesized with ImProm-II™ Reverse Transcription System (Promega, Madison, Wisconsin, USA) in a final volume of 20 µl in the presence of oligodT primer. The quantitative PCR (RT-qPCR) was performed using SYBR® Green I (Invitrogen) to detect double-strand cDNA synthesis on the 7500 Real-time PCR System (Applied Biosystems, CA, EUA). The primers used are shown in Table 1. All real-time assays were carried out in quadruplicate, and, in all cases, a reverse transcriptase negative control was included by substituting the templates for DNase/RNase-free distilled water in each PCR reaction. The beta-2-microglobulin (B2M) gene was used as the endogenous control. The efficiency for each sample was calculated using the software LinRegPCR version 2021.1 and the stability of the reference gene (M-value) and the optimal number of reference genes according to the pairwise variation (V) were analyzed by geNorm software. The relative expression levels were determined by the 2-ΔΔCq method.

Cell viability analysis

The compound 3-(4,5-dimethylthiazolyl)-2,5-diphenyltetrazolium bromide, inner salt (MTT) (CellTiter 96® Non-Radioactive Cell Proliferation Assay, Promega, USA) was used to quantify cell viability (3×10^4 per well in 96-well plate), according to the manufacturer's protocol. Briefly, U251 and LS12 cells were treated with MRS2179 (5, 10, 20, 50 µM) or ticagrelor (5, 10, 20, 50, 100, 200 µM) for 24 h. At the end of this period, 100 µl of the MTT solution (5 mg/ml) was added and incubated for 3 h. Formazan crystals were resuspended in 100 µl of dimethylsulfoxide (DMSO) and the absorbance was recorded at 595 nm with a 96-well plate reader (Spectra Max M2e, Soft Max®Pro 5, Molecular Devices). The cell viability in each well was expressed as a percentage compared to control cells.

Proliferation assay

U251 and LS12 cells were seeded (2×10^4 per well in 24-well plate) and after reaching 70% confluence, they were treated with ticagrelor (50 µM) and/or ADP (100 µM) for 24 h. After, cells were loosened with 200 µl of trypsin/EDTA solution, stained with trypan blue, and counted in an automated Cell Counter (Life Technologies, Waltham, MA, USA). The number of cells in the control group (untreated cells) was considered 100%.

Table 1 Primer sequences for the experiments included in this study

Gene	Primers efficiency	Forward primer	Reverse primer
P2RY1	1.7	5′-GGA TGC CAT GTG TAA ACT GC-3′	5′-GTA CAC CAC ACC GCT GTA CC-3′ [22]
P2RY2	2.0	5′-CAC CCG CAC CCT CTA CTA CT-3′	5′-CCT TGT AGG CCA TGT TGA TG-3′ [22]
P2RY4	2.0	5′-CCT GCC TGG TCA CTC TTG TT-3′	5′-CAG CTA TGG TGC GGA GAG AG-3′ [22]
P2RY6	1.9	5′-AGC TTC CTG CCT TTT CAC AT-3′	5′-AAA GGC CTC CAA TAC AGT GC-3′ [22]
P2RY11	-	5′-CAT GGC AGC CAA CGT CTC GG-3′	5′-GGG CCA CAG GAA GTC CCC CT-3′ [22]
P2RY12	2.0	5′-GCC TGG ATC CGT TCA TCT AT-3′	5′-GGG ACA GAG ATG TTG CAG AA-3′ [22]
P2RY13	2.1	5′-GAC TGC CGC CAT AAG AAG AC-3′	5′-CAG ATC TGT TGA AGC CTT GC-3′ [22]
P2RY14	1.8	5′-TCA CAG ATG AAG GCC TAG ACG CA-3′	5′-TGC CCA GTG AGC GTT TGT CGT-3′ [22]
*MMP2**	-	5′-CCC AGC GAC TCT AGA AAC ACA-3′	5′-GGG CCA CTA TTT CTC CGC TT-3′
*MMP9**	-	5′-CCT GGA GAC CTG AGA ACC AA-3′	5′-AGA TTT CGA CTC TCC ACG CA-3′
*β2-microglobulin**	-	5′-CTA TCC AGC GTA CTC CAA AG-3′	5′-ACA AGT CTG AAT GCT CCA CT-3′
B2M	2.0	5′-ACTGAATTCACCCCCACTGA-3′	5′-CCTCCATGATGCTGCTTACA-3′ [23]

The efficiencies of the primer sets are calculated individually for each sample ($n=4$) using the software LinRegPCR version 2021.1, and the efficiency shown in the table is an average of these efficiencies. *Designed by the authors

Clonogenic assay

GBM cells U251 and LS12 were plated at a density of 2×10^2 and 2×10^3 cells per well, respectively, in 12-well plates. Cells were treated with ticagrelor (50 µM) and/or ADP (100 µM) for 24 h. Then, the treatment was withdrawn, and the cells remained in culture for 10 days for the U251 and 21 days for LS12 cells. The medium was renewed every 2 days together with ADP (100 µM). At the end of the experiment, cells were washed with PBS, fixed with 4% formalin for 20 min, and stained with gentian violet for 10 min. Subsequently, cells were washed twice with PBS and stored at room temperature to dry. After 24 h, the images were obtained by the Cyber-shot DSC-W510 Sony Picture 12.1 megapixels, and the number of colonies was determined by the WCFI ImageJ (NIH) software. Results were shown as the absolute number of colonies.

Cell death and cell cycle analysis

U251 and LS12 cells were seeded (1×10^5 cells per well in a 24-well plate) and cultured for 24 h. Afterwards, cells were treated with ticagrelor (50 µM) for 24 h. At the end of the treatment, both the culture medium as well as the cells were harvested, centrifuged at 400 g for 6 min and washed with PBS (pH 7.4). Next, for cell death analysis, the cells were suspended in and quantified by annexin V-FITC–propidium iodide (PI) double staining, using Annexin V-FITC Apoptosis detection Kit I (BD, Biosciences, Mountain View, CA), according to the manufacturer's instructions. While, for cell cycle analysis, the cells were suspended in staining solution (0.5 mM) Tris–HCl (pH 7.6), 3.5 mM trisodium citrate, 0.1% NP 40 (v/v), 100 µg.mL^{-1} RNase and 50 µg.mL^{-1} PI at a concentration of 10^6 cells.mL^{-1}. Experiments were performed on FACS Calibur Flow Cytometer (BD Bioscienes), and the results were analyzed using FlowJo Software (Tree Star).

Autophagic analysis

The GBM cells (U251 and LS12) glioma cells were seeded (1×10^5 cells per well in a 24-well plate) and cultured for 24 h. Cells were treated with ticagrelor (50 µM) for 24 h. Autophagic cells were quantified by acridine orange staining 24 h after treatment, according to the manufacturer's instructions. The experiments were performed using the FACSCalibur flow cytometer (BD Biosciences) and the results were analyzed using the FlowJo software (Tree Star).

Nuclear morphology analysis (NMA)

The NMA assay was performed according to described by Filippi-Chiela et al. (2012) [24]. U251 and LS12 cells were seeded (10×10^3 cells per well in 24-well plate) for 24 h. GBM cells were then incubated with ticagrelor (50 µM) for 24 h. Next, cells were fixed with 4% formaldehyde for 20 min, and staining with Hoechst 33,342 (Sigma-Aldrich Canada) at a 1:1000 dilution in PBS. Photographs were taken under an inverted microscope at 100× magnification and analyzed. Data are presented as area versus nuclear irregularity index (NII) graphs.

Wound healing assay

The ability of cells to migrate in monolayer (2D) was investigated using the wound healing assay. Cells were plated in a 12-well plate (1×10^5) with 5% FBS and kept for 24 h. Then, using a p200 pipette tip, a straight line will be made at the bottom of the well, to mimic a situation of cell injury. Then, cells were treated with ticagrelor (50 µM) and/or ADP (100 µM). Image acquisition was made at 0 and 24 h with the aid of an inverted microscope, always in the same field. The images were analyzed with the help of the ImageJ package.

Spheroids migration assay

Spheroids were formed by depositing drops of LS12 cells (5×10^3 cells/20 µl) onto the bottom of the lid in a 48-wells plate, as previously described [25]. The lid was inverted onto the CMF-filled bottom chamber and incubated at 37 °C (5% CO_2 and 95% humidity atmosphere), for 4 days, until the cell aggregate was formed. LS12 Spheroids migration assay was performed according to Scheffel et al. (2022) [26]. The spheroids formed ($n = 4$) were dropped into a 48-well plate, previously treated with 0.1% gelatin for 2 h, and kept in medium with 2% FBS, then exposed to ticagrelor (20 µM) and/or ADP (20 µM). Images were recorded at 0, 24, and 48 h in an inverted microscope at 40× magnification and quantified using the Image-Pro 6 software.

Cell adhesion analysis

U251 and LS12 cells were seeded (4×10^4) in 200 µl of final volume for 1 h and exposed to ticagrelor (50 µM) and/or ADP (100 µM) alone and in association and maintained under ideal growing conditions. After 1 h, cells were washed with PBS and fixed in 4% formalin with 50 µl per well for 10 min. After the formalin was removed, the cells were stained with crystal violet diluted in 20% methanol for another 10 min. After the time, the dye was removed and the cells were washed with PBS and the formed crystals were eluted in 10% acetic acid for further reading in a spectrophotometer (Spectra Max M2e, Soft Max® Pro 5, Molecular Devices) at 595 nm.

ADPase activity

Cells were seeded (5×10^4) in a 24-well plate and after 48 h of cultivation, when in semi-confluency, they were treated with ticagrelor (50 µM) for 24 h. Cells were washed with phosphate-free incubation medium containing 20 mM Hepes buffer, 5.0 mM $CaCl_2$, KCl, 120 mM NaCl, 10 mM glucose, and pH 7.4. Cells were incubated in the same medium as described above, containing 1 mM ADP as a substrate. After 30 min, the reaction was stopped by withdrawing an aliquot of 150 µl which was transferred to tubes containing 150 µl of 10% trichloroacetic acid (TCA) previously kept on ice. Inorganic phosphate (Pi) released was measured by the malachite green method [27], using KH_2PO_4 as a standard. The non-enzymatic Pi, released by the spontaneous hydrolysis of nucleotides in the cell-free incubation medium, was subtracted from the total Pi released during the incubation. Specific activity was expressed as nmol Pi/min/mg protein.

Protein determination

After the enzymatic assay, cells in the 24-well plates were dried, solubilized with 100 µl NaOH (1.0 M), and kept in a freezer overnight. Subsequently, they were thawed, homogenized and then a sample of 50 µl was collected, whose amount of protein was determined by the Coomassie Blue method [28], using bovine serum albumin as a standard.

Statistical analysis

All data were expressed as mean ± standard deviation (SD) from at least three independent experiments. Data were analyzed by analysis of variance (ANOVA) one-way followed by Tukey's post hoc test or two-way followed by Bonferroni's post hoc test, or by Student's *t*-test using GraphPad Software (San Diego, CA, USA). p values < 0.05 were taken to indicate statistical significance.

Results

Characterization of P2Y receptors expression in human GBM

Initially, with the aim of comparing the expression of the P2Y receptors family ($P2Y_1$, $P2Y_2$, $P2Y_4$, $P2Y_6$, $P2Y_{11}$, $P2Y_{12}$, $P2Y_{13}$, and $P2Y_{14}$) in human GBM cells (U251 and LS12), we performed a screening of all P2YR receptors using the qRT-PCR assay. According to the data presented in Table 2, there was no difference in relation to the expression of $P2Y_1$, $P2Y_4$, $P2Y_{12}$, and $P2Y_{13}$ receptors between U251 and LS12. The results showed that $P2Y_2$ and $P2Y_{14}$ receptors are expressed only in patient-derived cells LS12. The $P2Y_6$ receptor demonstrated different patterns of expression (low and moderate) between cells. $P2Y_{11}$ receptor expression was not detected in any of the cells tested (Table 2). Besides, we analyzed the $P2Y_{12}$ expression level in TCGA cohorts comparing low- and high-grade gliomas (LGG and GBM) with different tumor types. As shown in Supplementary Fig. 1, both types of gliomas showed a higher expression of $P2Y_{12}$ when compared to the other tumors. Further analysis evaluating the effect $P2Y_{12}$ receptor expression level on glioma patients' survival showed no differences between high and low-medium P2YR12 expression in the survival probability of low grade and GBM patients (data not shown).

Table 2 P2YR gene expression in human glioblastoma cells

Receptor	U251	LS12
$P2Y_1$	10.56	5.13
$P2Y_2$	Absent	1.61
$P2Y_4$	0.63	0.43
$P2Y_6$	1.02	0.95
$P2Y_{11}$	Absent	Absent
$P2Y_{12}$	0.60	0.65
$P2Y_{13}$	0.58	0.42
$P2Y_{14}$	Absent	5.47

The relative mRNA expression compared to B2M expression

$P2Y_{12}$ receptor antagonism reduced the cell viability and proliferation in GBM cells

Since $P2Y_1$ and $P2Y_{12}$ receptors have the ADP as an endogenous ligand, we carried out a series of experiments to evaluate the effect of the selective antagonists of these receptors on mitochondrial activity through MTT assay. Treatment with the $P2Y_1$ receptor antagonist, MRS2179, for 24 h did not change cell viability at all concentrations tested (5–50 µM), thus indicating that $P2Y_1$ is not involved in the proliferation events of GBM cells under the conditions tested (Fig. 1A and B).

To assess the involvement of the $P2Y_{12}$ receptor in the cell viability, the patient-derived cells LS12 and a GBM cell line U251 were treated for 24 h with the selective antagonist, ticagrelor, and the MTT assay was performed. As shown in Fig. 1C and D, there was a reduction ($p < 0.001$) in cell viability in the cells tested beginning a 50 µM of the antagonist when compared to the vehicle control (DMSO). The values obtained from the IC_{50} were 117.2 µM for U251 and 82.5 µM for LS12 cells (Supplementary Fig. 2). To carry out the other experiments, we chose the concentration of 50 µM, which corresponds to the lowest effective concentration for tested cells.

Next, to assess the effect of the $P2Y_{12}$R antagonist on proliferation, human GBM cells were exposed to ticagrelor (50 µM) and ADP (100 µM), isolated or in association, for

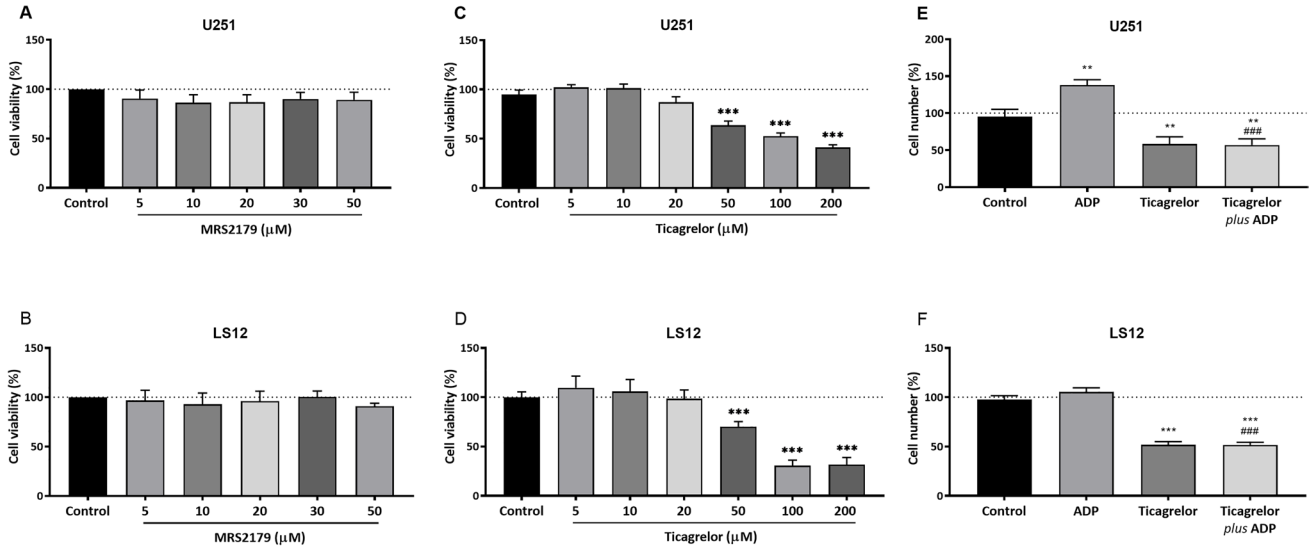

Fig. 1 Cell viability and proliferation of GBM cells. Effect of the $P2Y_1$ antagonist MRS2179 (5–50 μM for 24 h) and the $P2Y_{12}$ antagonist ticagrelor (5–200 μM for 24 h) were assessed using MTT assay for **A** and **C** U251 and **B** and **D** patient-derived GBM cells (LS12). For cell count, **E** U251 and **F** LS12 cells were treated with ticagrelor (50 μM) and/or ADP (100 μM) for 24 h. The cell number was expressed in % in relation to the control. Dimethylsulfoxide (DMSO) was used as a vehicle control. Values represent the mean ± standard deviation (SD) of three independent experiments performed in triplicate evaluated by one-way ANOVA followed by post hoc Tukey. *Means difference from the control group and # means difference from the ADP group. $^{*,\#}p<0.05$, $^{**,\#\#}p<0.01$, and. $^{***,\#\#\#}p<0.001$

24 h. After, the cell proliferation assay was performed. The results showed that ADP induced an increase in the number of cells in U251 cells ($p<0.001$). It should be noted that the patient-derived GBM cells did not show the same response to ADP (100 μM) isolated under the same treatment conditions, since it has a different time of growth. On the other hand, there was a reduction in the number of cells in the groups treated with ticagrelor (50 μM), U251 (34.2%; $p<0.01$), LS12 (44.2%; $p<0.001$), and with ticagrelor in association with ADP for U251 cells (36.3%; $p<0.01$), LS12 (44.6%; $p<0.001$) when compared to DMSO. The addition of ADP did not reverse the effect of ticagrelor after 24 h of treatment in any GBM cell type (Fig. 1E and F).

$P2Y_{12}$ receptor antagonism are related to a reduction in colony formation and ADPase activity of GBM cells

Following, to assess the long-term cell proliferation profile, we performed the colony formation assay for 10 days in U251 and, given the different growth characteristics of primary cells, for 21 days in LS12 cells. Both LS12 and U251 were exposed to ticagrelor (50 μM) and to ADP (100 μM), isolated or in combination, for 24 h. After this period, the groups that received ticagrelor were kept with the culture medium, which was renewed every 2 days, and the groups that received ADP continued to receive the treatment, also being renewed every 2 days. U251 cells showed a significant reduction in the number of colonies when treated with ticagrelor isolated (14.8 ± 6.3, $p<0.05$) or in association with ADP (15.3 ± 3.5, $p<0.05$) after 10 days (Fig. 2A and C). However, unlike the 24 h exposure to the agonist (ADP), there was no increase in the number of colonies in the commercial cell line. In contrast, patient-derived GBM cells exhibited an increase in the number of colonies formed when treated with ADP (11.0 ± 1.00, $p<0.001$) and there was a reduction in the number of colonies when cells were treated with the selective receptor antagonist $P2Y_{12}$ and in association with ADP (Fig. 2B and C).

To understand the ADP hydrolysis profile, the malachite green assay was performed, and it was investigated whether the $P2Y_{12}$ receptor blockade would be able to alter the ADPPase activity in different GBM cells. Interestingly, the treatment with ticagrelor (50 μM) reduced ADPase activity ($p<0.001$) in U251 (Fig. 2D). As seen in Fig. 2E, there were no changes in ADP hydrolysis after $P2Y_{12}$ receptor antagonism in the other glioma cells tested (LS12). It was observed that there is a significant difference in the basal hydrolysis profile between commercial or patient-derived GBM cells (data not shown), and the ADP hydrolysis was in order, LS12 > U251.

Changes in nuclear morphology were observed in GBM cells treated with ticagrelor

After having observed the decrease in the proliferation of GBM cells, a nuclear morphology analysis (NMA) was performed to assess the profile of the characteristics of the surviving tumor population after 72 h of exposure to the treatment.

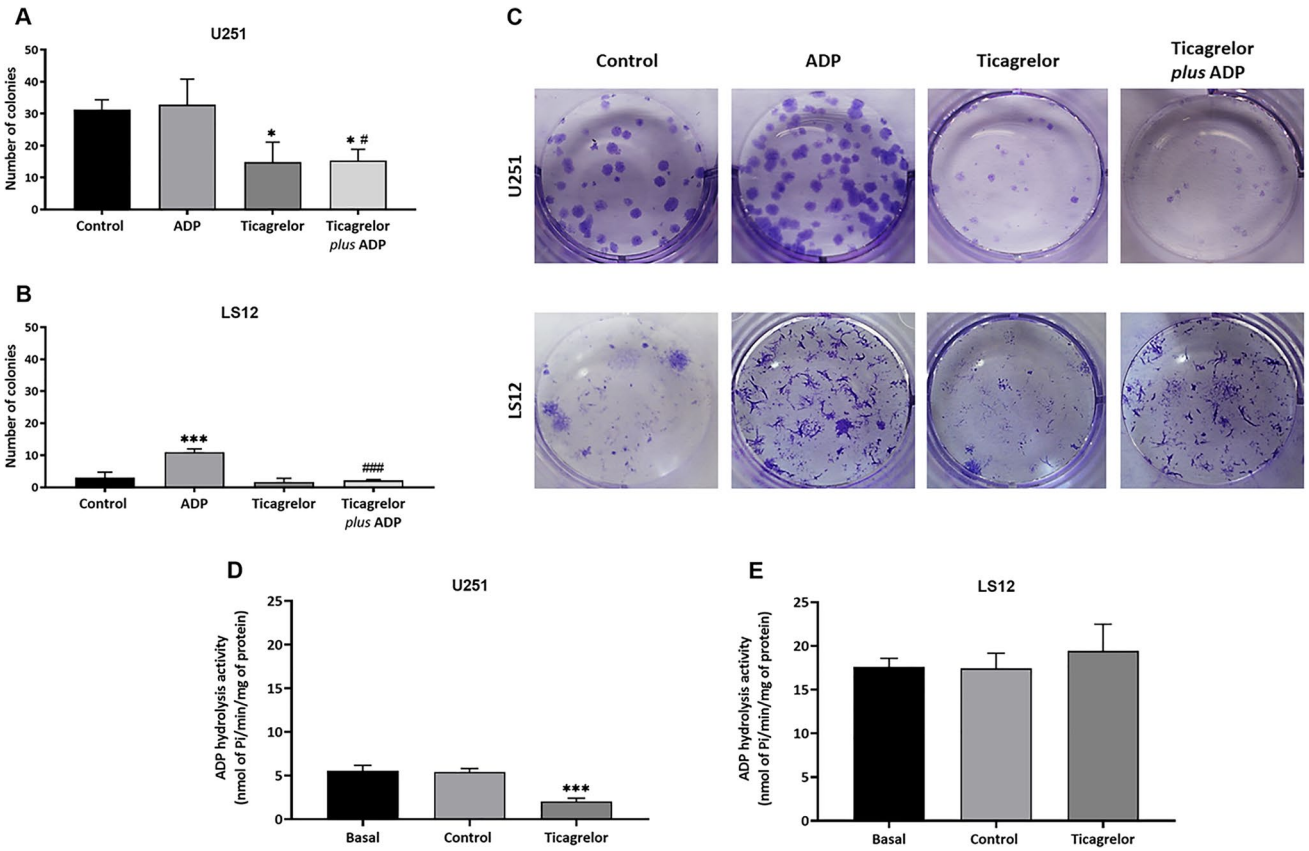

Fig. 2 Colony formation assay and ADP hydrolysis activity. Glioma cells **A** U251 and **B** LS12 were treated with ticagrelor (50 μM) and/or ADP (100 μM) for 24 h. In **C**, representative image of colony formation. The number of colonies is expressed as an absolute number. The ADP hydrolysis activity was measured using the malachite green method in **D** U251 and **E** LS12 cells treated with ticagrelor (50 μM) for 24 h. Values are represented as specific enzyme activity in nanomoles of inorganic phosphate per minute per milligram of protein. In (**F**), the comparison of basal hydrolysis between the GBM cell lines. Dimethylsulfoxide (DMSO) was used as a vehicle control. Values represent the mean ± standard deviation (SD) of three independent experiments performed in triplicate evaluated by one-way ANOVA followed by post hoc Tukey. *Means difference from the control group and # means difference from the ADP group. $^{*,\#}p < 0.05$, $^{**,\#\#}p < 0.01$, and. $^{***,\#\#\#}p < 0.001$

NMA is an analytical tool that enables the evaluation of characteristics associated with regularity and size (morphology) of the nuclei of adhered cells in culture [24] since various cellular devices, such as senescence, apoptosis, and mitotic catastrophe, can affect a nuclear morphology. U251 and LS12 cells were treated with ticagrelor (50 μM) for 24 h. After 72 h, the NMA was performed. Despite an expressive number of surviving cells with regular characteristics, these cells, when evaluated by clonogenic assay, are less active than untreated cells. The results were given by the distribution of the area of the nucleus in relation to the regularity index of the nuclei (NII), which allows classifying the nuclear morphology into six types of population (N, normal nuclei; I, irregular nucleus; LR, large and regular nucleus; LI, large and irregular nucleus; SR, small and regular nucleus; S, small nucleus; SI, small and irregular nucleus). The analysis demonstrated three predominant aspects of the distribution of morphological characteristics: normal (N), apoptotic (SR), and senescence (LR) cells. As shown in Fig. 3 and Table 3, U251 cells treated with the $P2Y_{12}R$ antagonist markedly nuclear altered when compared to the vehicle control, exhibiting an increase of about 15% of LR. The changes in the nucleus observed in the NMA analysis may be related to the morphological characteristics of senescent cells [29]. In contrast, LS12 cells did not show changes in the NMA. The population distribution of U251 cells presents a characteristic as more prominent cytoplasmic condensation when compared to LS12 cells (Table 3).

$P2Y_{12}$ receptor antagonism increased acridine orange staining in GBM cells

To evaluate the action of the $P2Y_{12}$ receptor antagonist in the cell cycle, the cells were analyzed at two different times. Initially, the protocol of treatment of cells with ticagrelor (50 μM) for 24 h and sequential analysis of the cell cycle through flow cytometry labeling with propidium iodide was

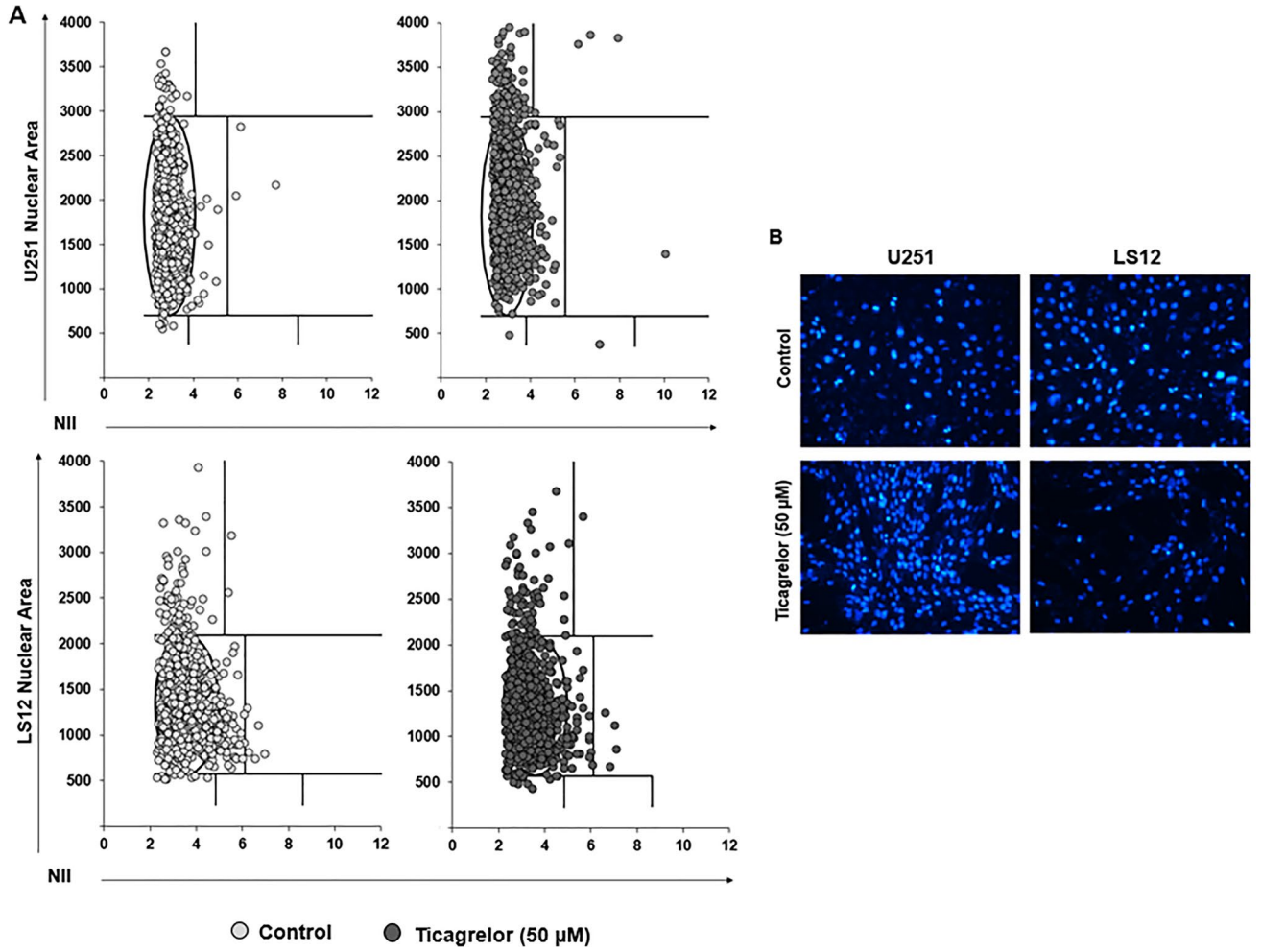

Fig. 3 Nuclear morphology analysis (NMA). U251 and LS12 cells were treated with ticagrelor (50 µM) for 24 h. In (**A**), the results are presented graphically and in N, normal nuclei; I, irregular core; LR, large and regular core; LI, large irregular core; SR, small, regular nucleus; S, small core; SI, small irregular nucleus (**B**) representative image

Table 3 Percentage and absolute distribution of morphological characteristics of the nuclei of U251 and LS12 cells

		Control		Ticagrelor (50 µM)	
Cells	Type of nuclei	%	*n*	%	*n*
U251	N	97.2	1307	90.6	1112
	SR	0.4	6	0.1	1
	LR	2.0	27	7.8	109
LS12	N	92.7	1110	89.7	911
	SR	0.6	9	1.3	13
	LR	5.9	67	7.0	71

N (normal); *SR* (apoptotic), and *LR* (senescence)

followed and no effect was observed (Fig. 4A and B). In view of the different characteristics of the cells and due to the morphological changes presented by the U251, it was decided to apply the same protocol used in the NMA analysis for the analysis of the cell cycle. Thus, cells were treated with ticagrelor for 24 h, and analysis was performed 72 h after treatment. As shown in Fig. 4C and D, changes were observed in the cell cycle progression of different cell types of GBM in these conditions, a decrease in G1 and enhancement in G2/M phases in U251, and an increase in the S phase of LS12.

To elucidate the data obtained in previous experiments, possible types of cell death related to treatment with the $P2Y_{12}R$ antagonist were evaluated using flow cytometry. U251 and LS12 cells were exposed to ticagrelor (50 µM) for 24 h for further analysis of markers of death by apoptosis and necrosis. As shown in Fig. 4E and F, none of the cell types showed a cell death profile of necrosis or apoptosis after treatment with ticagrelor, which led us to investigate whether the processes involved in decreasing cell number and formation of colonies could be related to autophagy and/or senescence. Since autophagy is a catabolic process in which the cell degrades organelles enhancing cellular

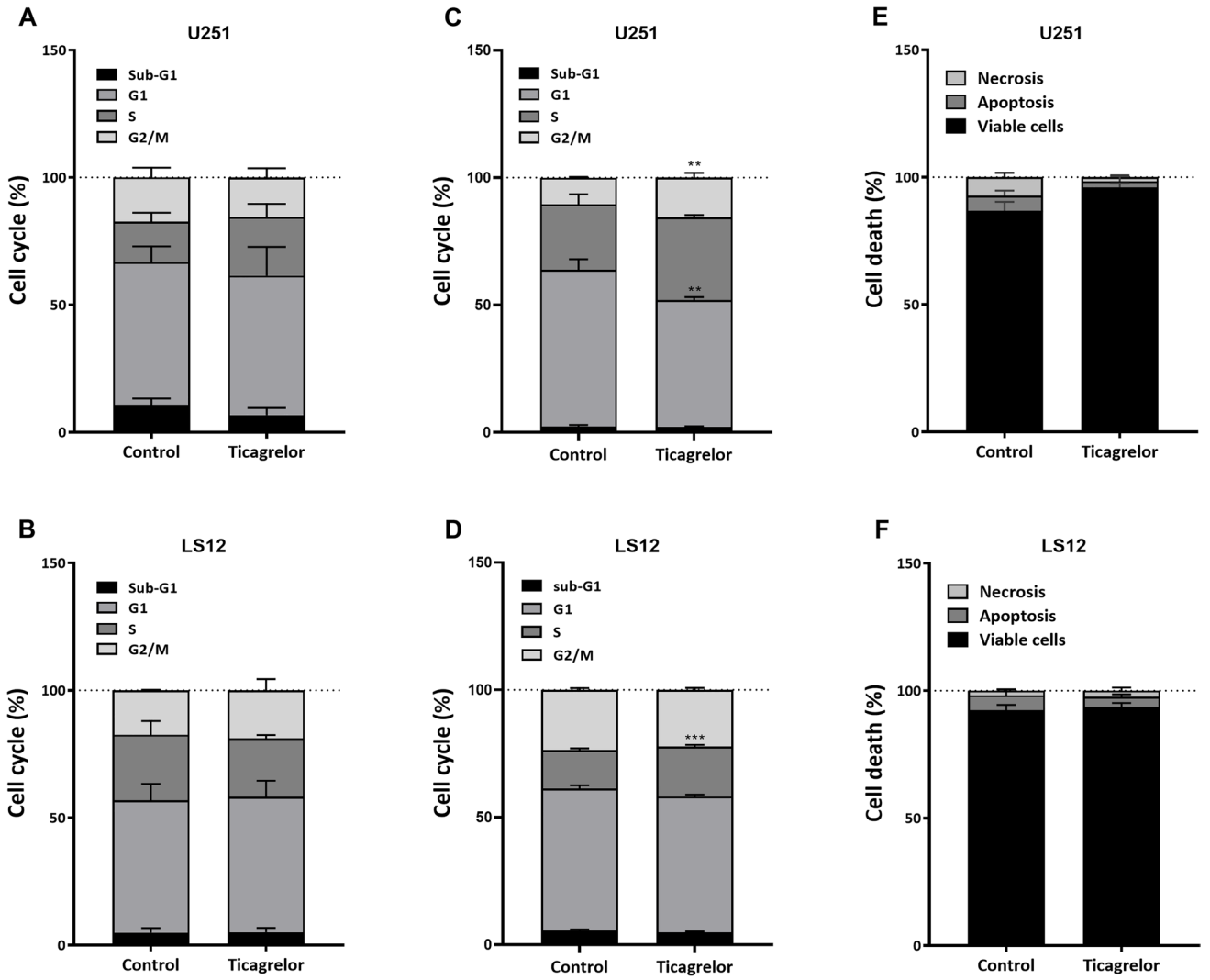

Fig. 4 Cell cycle and death analysis. For cell cycle analysis, **A** U251 and **B** LS12 were treated with ticagrelor (50 µM) for 24 and **C** U251 and **D** LS12 were treated with ticagrelor (50 µM) for 72 h. Cell cycle was analyzed by flow cytometry with propidium iodide labeling. Cell death was assessed with an annexin V kit using flow cytometry in **E** U251 and **F** LS12 treated with ticagrelor (50 µM) for 24 h. Dimethylsulfoxide (DMSO) was used as a vehicle control. Values represent the mean ± standard deviation (SD) of three independent experiments performed in triplicate evaluated by one-way ANOVA followed by post hoc Tukey. $^{*}p < 0.05$, $^{**}p < 0.01$,. $^{***}p < 0.001$

complexity when exposed to a type of injury, labeling with acridine orange was performed in both U251 and LS12 cultures. As observed in Fig. 5A, B, C, and D, the increase on the SSC axis indicates the cellular complexity increase, which is explained mainly by cellular autophagy induction after acute treatments. Figure 5C and F show the significant increase in acridine orange staining in relation to vehicle control suggesting the presence of autophagy in cells treated with the selective $P2Y_{12}$ receptor antagonist.

$P2Y_{12}$ blockade reduced the migratory profile of GBM cells

Cell migration is an important biological process in the growth and progression of GBM, which is one of the main characteristics that make treatment difficult due to the limited bioavailability of drugs in brain and tumor tissue. The migration assay, which uses the wound healing technique, assumes that an injury is made on the cell monolayer and from this "wound," the cells secrete several signaling chemokines to then close the formed gap. Thus, we continued with the assay in commercial cell line U251, while in the patient-derived cell culture we opted for the spheroids migration assay (3D), due to the different characteristics between the studied cells.

In this study, treatment with ticagrelor (50 µM) and ticagrelor *plus* ADP (100 µM) were able to reduce cell migration in 44.0% ($p < 0.01$) and 45.8% ($p < 0.01$), respectively, when compared to the control, in U251 cells. Treatment with ADP (100 µM) alone did not show significant

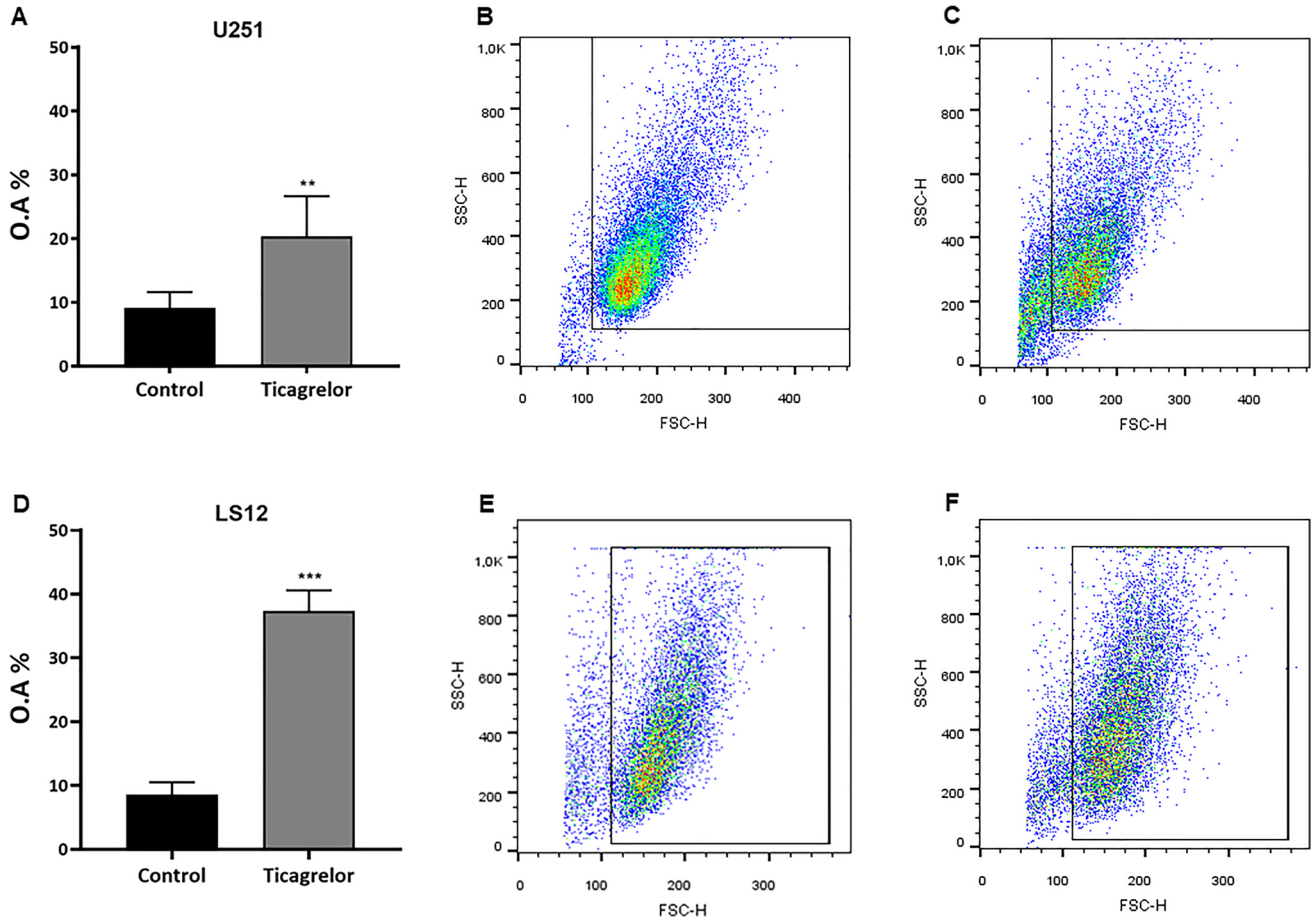

Fig. 5 Autophagy analysis. For authophagy analysis, **A** U251 and **D** LS12 cells were treated with ticagrelor (50 µM) for 24 h followed by acridine orange assay by flow cytometry. In **B** and **C** U251 and **E** and **F** LS12 representative SSC x FSC cytometry histograms of control and ticagrelor respectively. Dimethylsulfoxide (DMSO) was used as a vehicle control. Values represent the mean ± standard deviation (SD) of three independent experiments performed in triplicate evaluated by one-way ANOVA followed by post hoc Tukey. $^{*}p < 0.05$, $^{**}p < 0.01$, $^{***}p < 0.001$

differences in the healing process in either group (Fig. 6A or B). Differently from the 2D cell culture assays based on the principle of chemoattraction and migration in a monolayer, the evaluation model in 3D culture, used for LS12 cells, allows the assessment of migration based on the formation of a solid mass. The main advantage of this method is the representation of a model capable of simulating the physio morphological heterogeneity of solid tumors. Due to the different characteristics of the 2D and 3D migration models, the concentrations used were adapted to suit the 3D model. After the formation of the spheroid, LS12 cells were treated with ticagrelor (20 µM) and/or ADP (20 µM) and were photographed under an inverted microscope at times 0 h and 72 h. The results showed that ADP was able to increase the migratory profile of GBM cells, while ticagrelor, alone or associated with ADP, significantly reduced ($p < 0.001$) cell migration compared to the control group and ADP (Fig. 6C and D).

Subsequently, the cell adhesion assay was performed with a time of 1 h. Thus, the cells were exposed to ticagrelor (50 µM) and/or ADP (100 µM) and then seeded to adhere. After 1 h, cells were fixed and stained to quantify adhesion. The objective was to evaluate the interference capacity of the antagonism and agonism of the $P2Y_{12}R$ in the adhesion process of the studied GBM cells. As shown in Fig. 6E and F, treatments did not interfere with the adhesion capacity of any of the cells tested.

Considering the importance of metalloproteinases in the invasiveness and migration of CNS cells [30, 31], the action of ticagrelor on MMP-2 and MMP-9 expression was investigated. After treatment with ticagrelor (50 µM), we observed different behaviors between the studied cells. The U251 cell line showed a reduction in the expression of MMP-9 ($p < 0.05$), while in the patient-derived LS12, an increase in the expression of both MMP-2 and MMP-9 ($p < 0.05$) (Fig. 6G and H).

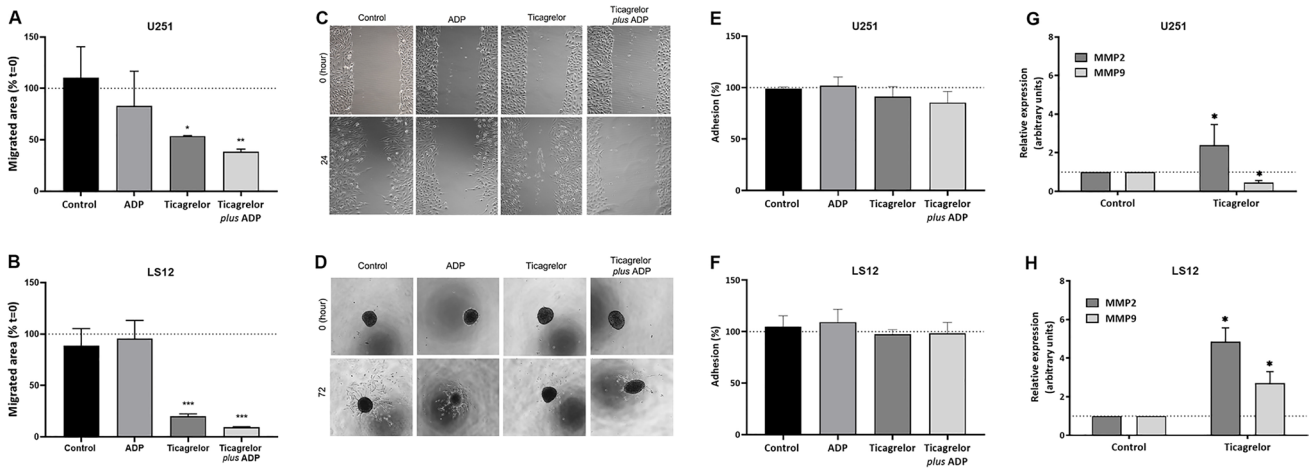

Fig. 6 Migration and adhesion profile of GBM cells. In the wound healing assay, **A** U251 cells were treated with ticagrelor (50 µM) and/or ADP (100 µM) for 24 h. Then, the cells were photographed at 0 h and 24 h and the cell migration space between the edges was measured. In (**B**), representative images of the cell migration process. For spheroid migration test, LS12 spheroids (**C**) were treated with ticagrelor (20 µM) and/or ADP (20 µM) for 48 h. Afterwards, they were photographed at 0 h and 72 h and the extent of migration was measured. In (**D**), representative image of the experiment. For the adherence assay, the cells **E** U251 and **F** LS12 cells were treated with ticagrelor (50 µM) and/or ADP (100 µM) and were seeded to adhere for 1 h. qPCR assay for metalloproteinases 2 and 9 was performed in **G** U251 and **H** LS12 cells treated with ticagrelor (50 µM) and the difference between the control group and the treated group was quantified. Dimethylsulfoxide (DMSO) was used as a vehicle control. Values represent the mean ± standard deviation (SD) of three independent experiments performed in triplicate analyzed by Student *t*-test. *Means difference from the control group and #means difference from the ADP group. $^{*,\#}p<0.05$, $^{**,\#\#}p<0.01$, and. $^{***,\#\#\#}p<0.001$

Discussion

The treatment of recurrent primary brain tumors is a challenge. It is associated with significant toxicities, and a balance must be achieved between local control and treatment of related morbidities and mortalities [32]. Due to the importance of the purinergic system in the progression of various tumors [33], especially gliomas, and the poor survival prognosis of this cancer type, we decided to investigate the effects of $P2Y_{12}R$ blockade by ticagrelor on glioma cells.

It is known that $P2RY_{12}$ high expression is associated with poor prognosis in diverse tumor types such as, glioma, colon, and non-small cancer (NSCLC) [34]. In this study, we showed that U251 and LS12 human GBM cells express the $P2Y_{12}R$. To evaluate the involvement of this receptor on GBM cells proliferation and viability, different concentrations of ticagrelor were tested. We showed that the treatment with ticagrelor decreased cell viability and cell number after 24 h of treatment in both cell cultures. Previous study showed that $P2Y_{12}R$-mediated proliferation activates the cascade of the ERK pathway in several cell types, such as smooth muscle cells and astrocytes [35]. Furthermore, when nucleotide degradation is blocked in C6 rat glioma cells, the availability of the agonist ADP, in the extracellular medium, activates the ERK 1/2 through a mechanism dependent on cascade RhoA/PKC/Raf1/MEK-dependent by binding to the $P2Y_{12}R$, increasing cell proliferation and decreasing cell differentiation [18, 35].

In this study, we also observed that ticagrelor can exert biological effects independently of cell stimulation by ADP. This could suggest that $P2Y_{12}$ receptor is constitutively activated following a possible release of ADP or the generation of extracellular ADP. Interestingly, a previous study has shown the effect of a potent inverse agonist in Chinese hamster ovary cells expressing a constitutively active chimeric $P2Y_{12}$ receptor [36]. The ATP/ADP proliferative effects have already been elucidated. In fact, Morrone et al. (2006) showed that when C6 glioma cells where implanted in an in vivo glioma model in association with the enzyme apyrase, which catalyzes the breakdown of ATP in AMP + inorganic phosphate, the glioma progression decreased [37]. In addition, it is known that ATP is capable of accumulating in the extracellular environment as consequence of nonspecific membrane damage or through specific permeation pathways [15, 38]. Also, ATP as well as other nucleotides and adenosine may induce glioma proliferation [39].

Moreover, Wink et al. (2003) have demonstrated that glioma cells exhibit altered extracellular ATP, ADP, and AMP catabolism, showing lower extracellular ATP and ADP hydrolysis rates when compared to extracellular AMP hydrolysis in relation to normal astrocytes, evidencing the glioma preference to keep the extracellular ATP and ADP [40]. Accordingly, the results obtained in this study confirmed the hypothesis of purinergic signaling in gliomas' growth, once the blockage of ADP signaling through the $P2Y_{12}R$ antagonist, ticagrelor, have culminated in antiproliferative effects. In fact, our results agree with Braganhol et al.

(2009) which showed that in vivo tumors implanted with C6 cells that overexpress NTPDase2 (accumulating ADP) were bigger than tumors from C6 wild type implantation. Furthermore, treatment with clopidogrel markedly reduced tumor size, malignity characteristics, angiogenesis, and the inflammatory process in C6-EYFP/NTPDase2-derived gliomas [41]. Other studies also demonstrated that the $P2Y_{12}$ antagonist, ticagrelor, has potential to reduce tumor growth in murine models of ovarian cancer [42], and in melanoma and breast cancer [43].

Herein, ticagrelor had slight or no cell cycle, apoptosis, or necrosis effects, and its antiproliferative effects were attributed to autophagy induction. Comparable results were obtained by Shchors et al. (2015), which showed that GBM cells may get into the autophagy process when exposed to a $P2Y_{12}R$ antagonist, ticlopidine, associated with imipramine [44]. Autophagy is a lysosome-dependent process that degrades organelles to establish cellular homeostasis, in response to damage, such as oxidative stress, nutrient deprivation, and injury to cellular DNA. Several genes control this pathway, including mTOR, PI3k/Akt and MAPK [45]. The inhibition of $P2Y_{12}R$ increases the levels of cAMP by upregulating adenylate cyclase leading to autophagic flux [44, 45]. It has been proposed that autophagy contributes to oncogene-induced cell death or senescence, two essential oncosupressive mechanisms. Here, we demonstrated that ticagrelor increased the percentage of AO-positive cells. Chemical-induced autophagy has a dual role in cancer cells: the one hand, can contribute to cell resistance and survival; on the other hand, it can contribute to the toxicity of treatments. Previously, it has been suggested that autophagy is involved on the degradation of oncogenic proteins, such as P53, p62, PML-RARA, and BCR-ABL1 [34]. According to Ma et al. (2013) autophagy is involved in the immune responses that prevent the establishing and multiplying of malignant cells. At least in some situations, dying malignant cells are capable of recruiting antigen-presenting cells (APCs) and other cellular components of the immune system, resulting in the elicitation of innate and/or adaptive antitumor immune responses [46]. Autophagy responses are essential for dying neoplastic cells to release ATP in optimal amounts, which not only recruits APCs through purinergic receptor P2Y but also triggers them to release immune stimulatory chemokines through purinergic receptor P2X7 [45]. Differently and interestingly, in our study, treatment with ticagrelor induced autophagy that culminates in GBM cell death.

The tumor-inhibiting role of autophagy in certain human cancers is increasingly being demonstrated. For example, in GBM patients, comparatively higher levels of autophagy are associated with better survival prognosis [47]. Moreover, autophagy is a process closely linked with intracellular calcium modulation and calcium balance between endoplasmic reticulum, mitochondria, and lysosome which could culminate in different cellular fate as cancer death as well as cancer progression depending on the other autophagy components expression and participation [48]. Furthermore, Shchors et al. (2015) have shown that thienopyridines associated with imipramine induce autophagy in GBM cells, resulting in the reduction of proliferative index, although the role of autophagy in cancer progression is complex [44]. For that, the outcome of autophagy activation in cancer cells depends on the stage of the disease progression, cell type, oncogenic drivers, and the intensity of the activating signal. In addition to inducing autophagy, our data showed that ticagrelor also reduced the migratory profile of GBM cells, which is one of the patient's treatments challenges. Normally, the $P2Y_{12}$ blockade and the reduction of migration are linked with MMP-2 and MMP-9 expression decrease; nonetheless, autophagy has been described to involve the increase of MMPs [49–51], particularly of MMP-9 [51], which agrees with our results.

In conclusion, although other studies are needed to confirm this hypothesis, our results support the idea that the $P2Y_{12}R$ modulation can reduce glioma proliferation, migration and could be considered a potential pharmacological target to treat gliomas.

Supplementary Information The online version contains supplementary material available at https://doi.org/10.1007/s11302-022-09888-w.

Author contribution PV performed cell growth, cell viability, cell counting, clonogenic assay, drug treatments, performed data analysis, and drafting of the manuscript. TBS performed 3D cell culture and spheroid migration assay, performed data analysis, and editing the manuscript. FMD and ECF performed NMA assay and performed data analysis. LR performed the PCR and flow cytometry assays, performed data analysis, and editing the manuscript. NG, LWK, MRB, and ARC also performed the PCR assay. GL has been collaborating with patient derived GBM cells. GFL performed the TCGA data selection and analysis. FF and AFD performed the flow cytometry assay and the Flow Jow analysis, and FF also provided the reagents for the flow cytometry assay. FBM wrote and guided this manuscript, was responsible for data analysis, and purchased the reagents. All the authors read and approved the final manuscript.

Funding We would like to acknowledge ongoing research funding from Coordenação de Aperfeiçoamento de Pessoal de Nivel Superior – Brasil [CAPES, Finance Code 001], Conselho Nacional de Desenvolvimento Científico e Tecnológico [CNPq, Project N° 310317/2018–5] and Financiadora de Estudos e Projetos [FINEP Research Grant "Implantação, Modernização e Qualificação de Estrutura de Pesquisa da PUCRS" (PUCRSINFRA) #01.11.0014–00].

Data availability Not applicable.

Declarations

Ethics approval Ethical Committee approval protocol at UFRGS: 420.856 and at PUCRS: 429.849.

Informed consent This study was conducted in accordance with the appropriate guidelines and ethical protocols and after obtaining informed consent from the patient.

Conflict of interest The authors declare no competing interests.

References

1. Alifieris C, Trafalis DT (2015) Glioblastoma multiforme: pathogenesis and treatment. Pharmacol Ther 152:63–82. https://doi.org/10.1016/j.pharmthera.2015.05.005
2. Jain KK (2018) A critical overview of targeted therapies for glioblastoma. Front Oncol 8:419
3. Ferlay J, Parkin DM, Steliarova-Foucher E (1990) Estimates of cancer incidence and mortality in Europe in 2008. Eur J Cancer Oxf Engl 2010(46):765–781. https://doi.org/10.1016/j.ejca.2009.12.014
4. Weller M, Wick W, Aldape K, Brada M, Berger M, Pfister SM et al (2015) Glioma. Nat Rev Dis Primer 1:15017. https://doi.org/10.1038/nrdp.2015.17
5. Claes A, Idema AJ, Wesseling P (2007) Diffuse glioma growth: a guerilla war. Acta Neuropathol (Berl) 114:443–458. https://doi.org/10.1007/s00401-007-0293-7
6. Verhaak RGW, Hoadley KA, Purdom E, Wang V, Qi Y, Wilkerson MD et al (2010) Integrated genomic analysis identifies clinically relevant subtypes of glioblastoma characterized by abnormalities in PDGFRA, IDH1, EGFR, and NF1. Cancer Cell 17:98–110. https://doi.org/10.1016/j.ccr.2009.12.020
7. Wolf KJ, Chen J, Coombes J, Aghi MK, Kumar S (2019) Dissecting and rebuilding the glioblastoma microenvironment with engineered materials. Nat Rev Mater 4:651–668. https://doi.org/10.1038/s41578-019-0135-y
8. Stupp R, Mason WP, van den Bent MJ, Weller M, Fisher B, Taphoorn MJB et al (2005) Radiotherapy plus concomitant and adjuvant temozolomide for glioblastoma. N Engl J Med 352:987–996. https://doi.org/10.1056/NEJMoa043330
9. Chang L, Su J, Jia X, Ren H (2014) Treating malignant glioma in Chinese patients: update on temozolomide. OncoTargets Ther 7:235–244. https://doi.org/10.2147/OTT.S41336
10. Hoelzinger DB, Demuth T, Berens ME (2007) Autocrine factors that sustain glioma invasion and paracrine biology in the brain microenvironment. J Natl Cancer Inst 99:1583–1593. https://doi.org/10.1093/jnci/djm187
11. Morrone FB, Vargas P, Rockenbach L, Scheffel TB (2021) P2Y12 purinergic receptor and brain tumors: implications on glioma microenvironment. Molecules 26:6146. https://doi.org/10.3390/molecules26206146
12. Praetorius HA, Leipziger J (2010) Intrarenal purinergic signaling in the control of renal tubular transport. Annu Rev Physiol 72:377–393. https://doi.org/10.1146/annurev-physiol-021909-135825
13. Ohta A (2016) A Metabolic immune checkpoint: adenosine in tumor microenvironment. Front Immunol 7. https://doi.org/10.3389/fimmu.2016.00109
14. Morrone FB, Gehring MP, Nicoletti NF (2016) Calcium channels and associated receptors in malignant brain tumor therapy. Mol Pharmacol 90:403–409. https://doi.org/10.1124/mol.116.103770
15. Di Virgilio F, Sarti AC, Falzoni S, De Marchi E, Adinolfi E (2018) Extracellular ATP and P2 purinergic signalling in the tumour microenvironment. Nat Rev Cancer 18:601–618. https://doi.org/10.1038/s41568-018-0037-0
16. Yanachkov IB, Chang H, Yanachkova MI, Dix EJ, Berny-Lang MA, Gremmel T et al (2016) New highly active antiplatelet agents with dual specificity for platelet P2Y1 and P2Y12 adenosine diphosphate receptors. Eur J Med Chem 107:204–218. https://doi.org/10.1016/j.ejmech.2015.10.055
17. Haynes SE, Hollopeter G, Yang G, Kurpius D, Dailey ME, Gan W-B et al (2006) The P2Y12 receptor regulates microglial activation by extracellular nucleotides. Nat Neurosci 9:1512–1519. https://doi.org/10.1038/nn1805
18. Krzeminski P, Misiewicz I, Pomorski P, Kasprzycka-Guttman T, Barańska J, Brańska J (2007) Mitochondrial localization of P2Y1, P2Y2 and P2Y12 receptors in rat astrocytes and glioma C6 cells. Brain Res Bull 71:587–592. https://doi.org/10.1016/j.brainresbull.2006.11.013
19. Ballerini P, Dovizio M, Bruno A, Tacconelli S, Patrignani P (2018) P2Y12 receptors in tumorigenesis and metastasis. Front Pharmacol 0. https://doi.org/10.3389/fphar.2018.00066
20. Birkeland K, Parra D, Rosenstein R (2010) Antiplatelet therapy in acute coronary syndromes: focus on ticagrelor. J Blood Med 1:197–219. https://doi.org/10.2147/JBM.S9650
21. Kipper FC, Silva AO, Marc AL, Confortin G, Junqueira AV, Neto EP et al (2018) Vinblastine and antihelmintic mebendazole potentiate temozolomide in resistant gliomas. Invest New Drugs 36:323–331. https://doi.org/10.1007/s10637-017-0503-7
22. Zaparte A, Cappellari AR, Brandão CA, de Souza JB, Borges TJ, Kist LW, Bogo MR, Zerbini LF, Ribeiro Pinto LF, Glaser T, Gonçalves MCB, Naaldijk Y, Ulrich H, Morrone FB (2021) P2Y2 receptor activation promotes esophageal cancer cells proliferation via ERK1/2 pathway. Eur J Pharmacol 891:173687. https://doi.org/10.1016/j.ejphar.2020.173687
23. Rho HW, Lee BC, Choi ES, Choi IJ, Lee YS, Goh SH (2010) Identification of valid reference genes for gene expression studies of human stomach cancer by reverse transcription-qPCR. BMC Cancer 10:240. https://doi.org/10.1186/1471-2407-10-240
24. Filippi-Chiela EC, Oliveira MM, Jurkovski B, Callegari-Jacques SM, da Silva VD, Lenz G (2012) Nuclear morphometric analysis (NMA): screening of senescence, apoptosis and nuclear irregularities. PLoS One 7:e42522. https://doi.org/10.1371/journal.pone.0042522
25. Foty R (2011) A Simple Hanging Drop Cell Culture Protocol for Generation of 3D Spheroids. J Vis Exp JoVE. https://doi.org/10.3791/2720
26. Scheffel TB, Rockenbach L, Cruz FF, Kist LW, Bogo MR, Scholl JN et al (2022) Inhibition of ATP hydrolysis as a key regulator of temozolomide resistance and migratory phenotype of glioblastoma cells. Biochem Biophys Res Commun. https://doi.org/10.1016/j.bbrc.2022.02.062
27. Ekman P, Jäger O (1993) Quantification of subnanomolar amounts of phosphate bound to seryl and threonyl residues in phosphoproteins using alkaline hydrolysis and malachite green. Anal Biochem 214:138–141. https://doi.org/10.1006/abio.1993.1468
28. Bradford MM (1976) A rapid and sensitive method for the quantitation of microgram quantities of protein utilizing the principle of protein-dye binding. Anal Biochem 72:248–254. https://doi.org/10.1006/abio.1976.9999
29. Demuth T, Berens ME (2004) Molecular mechanisms of glioma cell migration and invasion. J Neurooncol 70:217–228. https://doi.org/10.1007/s11060-004-2751-6
30. Uhm JH, Dooley NP, Villemure JG, Yong VW (1996) Glioma invasion in vitro: regulation by matrix metalloprotease-2 and protein kinase C. Clin Exp Metastasis 14:421–433. https://doi.org/10.1007/BF00128958
31. Yong VW, Power C, Forsyth P, Edwards DR (2001) Metalloproteinases in biology and pathology of the nervous system. Nat Rev Neurosci 2:502–511. https://doi.org/10.1038/35081571
32. Mallick S, Benson R, Hakim A, Rath GK (2016) Management of glioblastoma after recurrence: a changing paradigm. J Egypt Natl Cancer Inst 28:199–210. https://doi.org/10.1016/j.jnci.2016.07.001

33. Burnstock G, Di Virgilio F (2013) Purinergic signalling and cancer. Purinergic Signal 9:491–540. https://doi.org/10.1007/s11302-013-9372-5
34. Hollopeter G, Jantzen HM, Vincent D, Li G, England L, Ramakrishnan V et al (2001) Identification of the platelet ADP receptor targeted by antithrombotic drugs. Nature 409:202–207. https://doi.org/10.1038/35051599
35. Van Kolen K, Slegers H (2006) Atypical PKCζ is involved in RhoA-dependent mitogenic signaling by the P2Y12 receptor in C6 cells. FEBS J 273:1843–1854. https://doi.org/10.1111/j.1742-4658.2006.05205.x
36. Ding Z, Kim S, Kunapuli SP (2006) Identification of a potent inverse agonist at a constitutively active mutant of human P2Y12 receptor. Mol Pharmacol 69(1):338–345. https://doi.org/10.1124/mol.105.014654
37. Morrone FB, Oliveira DL, Gamermann P, Stella J, Wofchuk S, Wink MR et al (2006) In vivo glioblastoma growth is reduced by apyrase activity in a rat glioma model. BMC Cancer 6:226. https://doi.org/10.1186/1471-2407-6-226
38. Yegutkin GG (2008) Nucleotide- and nucleoside-converting ectoenzymes: Important modulators of purinergic signalling cascade. Biochim Biophys Acta 1783:673–694. https://doi.org/10.1016/j.bbamcr.2008.01.024
39. Morrone FB, Jacques-Silva MC, Horn AP, Bernardi A, Schwartsmann G, Rodnight R et al (2003) Extracellular nucleotides and nucleosides induce proliferation and increase nucleoside transport in human glioma cell lines. J Neurooncol 64:211–218. https://doi.org/10.1023/a:1025699932270
40. Wink MR, Lenz G, Braganhol E, Tamajusuku ASK, Schwartsmann G, Sarkis JJF et al (2003) Altered extracellular ATP, ADP and AMP catabolism in glioma cell lines. Cancer Lett 198:211–218. https://doi.org/10.1016/S0304-3835(03)00308-2
41. Braganhol E, Morrone FB, Bernardi A, Huppes D, Meurer L, Edelweiss MIA et al (2009) Selective NTPDase2 expression modulates in vivo rat glioma growth. Cancer Sci 100:1434–1442. https://doi.org/10.1111/j.1349-7006.2009.01219.x
42. Cho MS, Noh K, Haemmerle M, Li D, Park H, Hu Q, Hisamatsu T, Mitamura T, Mak SLC, Kunapuli S, Ma Q, Sood AK, Afshar-Kharghan V (2017) Role of ADP receptors on platelets in the growth of ovarian cancer. Blood 130(10):1235–1242. https://doi.org/10.1182/blood-2017-02-769893
43. Gebremeskel S, LeVatte T, Liwski RS, Johnston B, Bezuhly M (2015) The reversible P2Y12 inhibitor ticagrelor inhibits metastasis and improves survival in mouse models of cancer. Int J Cancer 136:234–240. https://doi.org/10.1002/ijc.28947
44. Shchors K, Massaras A, Hanahan D (2015) Dual targeting of the autophagic regulatory circuitry in gliomas with repurposed drugs elicits cell-lethal autophagy and therapeutic benefit. Cancer Cell 28:456–471. https://doi.org/10.1016/j.ccell.2015.08.012
45. Vessoni AT, Filippi-Chiela EC, Menck CF, Lenz G (2013) Autophagy and genomic integrity. Cell Death Differ 20:1444–1454. https://doi.org/10.1038/cdd.2013.103
46. Ma Y, Galluzzi L, Zitvogel L, Kroemer G (2013) Autophagy and cellular immune responses. Immunity 39:211–227. https://doi.org/10.1016/j.immuni.2013.07.017
47. Escamilla-Ramírez A, Castillo-Rodríguez RA, Zavala-Vega S, Jimenez-Farfan D, Anaya-Rubio I, Briseño E et al (2020) Autophagy as a potential therapy for malignant glioma. Pharmaceuticals 13:156. https://doi.org/10.3390/ph13070156
48. Filippi-Chiela EC, Viegas MS, Thomé MP, Buffon A, Wink MR, Lenz G (2016) Modulation of autophagy by calcium signalosome in human disease. Mol Pharmacol 90:371–384. https://doi.org/10.1124/mol.116.105171
49. Pratt J, Roy R, Annabi B (2012) Concanavalin-A-induced autophagy biomarkers requires membrane type-1 matrix metalloproteinase intracellular signaling in glioblastoma cells. Glycobiology 22(9):1245–1255. https://doi.org/10.1093/glycob/cws093
50. Desjarlais M, Pratt J, Lounis A, Mounier C, Haidara K, Annabi B (2014) Tetracycline derivative minocycline inhibits autophagy and inflammation in concanavalin-a-activated human hepatoma cells. Gene Regul Syst Bio 8:63–73. https://doi.org/10.4137/GRSB.S13946
51. Martinelli S, Anderzhanova EA, Bajaj T, Wiechmann S, Dethloff F, Weckmann K, Heinz DE, Ebert T, Hartmann J, Geiger TM, Döngi M, Hafner K, Pöhlmann ML, Jollans L, Philipsen A, Schmidt SV, Schmidt U, Maccarrone G, Stein V, Hausch F, Turck CW, Schmidt MV, Gellner AK, Kuster B, Gassen NC (2021) Stress-primed secretory autophagy promotes extracellular BDNF maturation by enhancing MMP9 secretion. Nat Commun 12(1):4643. https://doi.org/10.1038/s41467-021-24810-5